Flexibility and Curvature of Duplex DNA Containing Mismatched Sites as a Function of Temperature†

Vasilios M. Marathias, Bozidar Jerkovic, Haribabu Arthanari, and Philip H. Bolton*

Chemistry Department, Wesleyan University, Middletown, Connecticut 06459

Received July 20, 1999; Revised Manuscript Received September 23, 1999

ABSTRACT: The flexibility and curvature of duplex DNAs containing mismatched sites have been monitored as a function of temperature. The diffusion coefficients are dependent on the flexibility and the curvature of the DNA, and these have been determined by NMR-based methods. The diffusion coefficients, D, depend on a Boltzmann term and the viscosity of the solvent, η, which is also temperature dependent. To analyze the temperature dependence of the diffusion results, the shape function, $S_f = \eta D/T$, is used. The shape functions do not have the viscosity and temperature dependence of the diffusion coefficients. The presence of mismatched sites significantly enhances the shape function of duplex DNA at all temperatures examined. The observed increases in the shape functions are attributed to the mismatched sites acting as localized flexible joints. The results on the temperature dependence of the shape functions, the optical absorbance, and the proton chemical shifts indicate that local melting at, and adjacent to, mismatched site occurs at a lower temperature than the overall melting of the duplexes. The localized melting gives rise to a considerable increase in the shape function. The contribution of the curvature of the mismatched sites to the enhanced diffusion has been examined. A DNA with mismatches that are in phase with respect to the helical repeat and a DNA which has the mismatches out of phase with respect to the helical repeat have been examined. The results indicate that mismatched sites have modest curvature.

The biological and physical consequences of mismatched sites in DNA have been extensively examined by many different approaches (*1−14*). It is known that mismatched sites can lead to stable mutations and to errors in transcription (*15, 16*). The repair of mismatched sites has been studied, and some cytotoxic anti-cancer agents disrupt mismatch repair (*15−19*). There is also considerable information on the effects of mismatched sites on the structure and the stability of duplex DNA (*1−14*). We have recently proposed that the flexibility of damaged DNA, including mismatched sites, can be used as a global means of recognition (*20*).

All possible mismatches can occur naturally. The dG-dU wobble pairing is perhaps the most common in vivo and arises from the spontaneous deamination of cytosine, and the dG-dT wobble pairing can arise from misreplication (*21*). Mismatched sites have been found to have a considerable range of effects on DNA structure (*3, 6−11, 13, 22*) and stabilities (*12−14, 23*) of DNA. The smallest disruptions appear to occur with the wobble, dG-dT/U, mispairs, and the most destabilizing tend to be the sterically unfavorable purine-purine mismatches (*14*). The mismatch repair system can apparently recognize and repair all mismatched sites (*15−19*).

The presence of mismatched sites is thought to induce structural changes that are localized to the region within two residues of the mispair (*2, 3, 6−14, 22, 24*). The presence of mismatched sites may also alter the flexibility and curvature of DNA and thus alter DNA−protein interactions, including recognition (*25−28*). It has been shown that the affinity of a transcription factor for DNA increases in the presence of a mismatched site. The transcription factor bends the DNA, and the increase in flexibility, due to the presence of the mismatched site, lowers the energy needed to adopt the bound state and increases the binding coefficient (*25−27*). Similarly, the assembly of nucleosomes depends on the flexibility and curvature of DNA (*29, 30*). Flexible sites may also act as universal joints to allow contact between proteins bound at distant cis elements (*31*).

The overall flexibility of DNAs containing a triple mismatch has been studied by examining the rate of cyclization by ligation (*32*) and the mobility of the residues involved in single mismatches by NMR-based methods (*9*). Triple mismatches considerably enhance the rate of cyclization (*32*). This has been taken as evidence that triple mismatched sites increase the local flexibility of DNA (*32*). The residues in dC-dC and in dC-dT mismatches have been found to be locally mobile by NMR methods (*9*). We recently examined the effects of the presence of single and triple mismatched sites on the rate of diffusion of DNA and found that the presence of mismatched sites increases the overall flexibility of DNA (*20*).

To more fully understand the effects of mismatched sites, additional information on the temperature dependence of the

```
ACAGGACCGCGATACGCCGGAACGA
TGTCCTGGCGCTATGCGGCCTTGCT
```
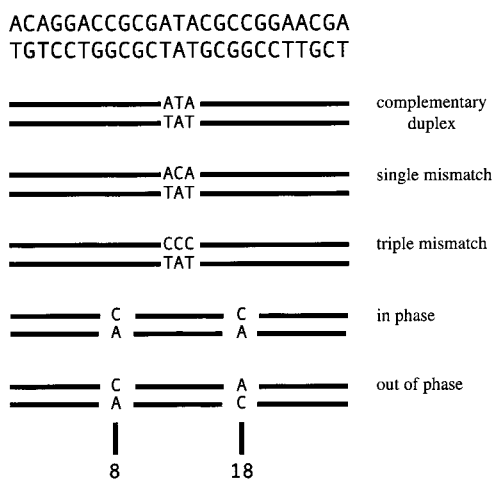

FIGURE 1: Complementary and mismatched sequences used are depicted. The fully complementary 25mer sequence is shown at the top. Below it are shown the positions of the single and triple mismatches as well as the positions of the mismatches which are in or out of phase with respect to the helical repeat.

flexibility and curvature has been obtained and compared to the overall melting of the DNA. The model put forth here is that the increase in flexibility is primarily due to the localized melting of the DNA near the mismatched site. Several features of this proposed model are tested here.

The temperature dependence is also needed in order to be able to estimate the energy associated with the curvature and flexibility of mismatched DNAs. We have recently proposed that much of the global recognition of damaged DNA can be based on the flexibility of the damaged DNA (*20*). Recognition, in this model, is based on the ease with which the DNA can be bent to form a suitable protein−DNA complex that may then interact with additional proteins. A significant portion of the recognition may be based on the interaction with these additional proteins. This mode of action can be used for global recognition in cell cycle regulation, in DNA repair, and in other biological systems. The model requires that the free energy needed for the bending of most damaged DNAs is sufficiently lower than that of normal DNA to allow for discrimination between them. It is known that duplex DNA can be bent by proteins (*33, 34*) so the total energy needed to bend damaged DNA is accessible to biological systems.

The enhanced diffusion is proposed to be due to the localized flexibility of the mismatched site at low temperatures and to melting at, and adjacent to, the mismatched sites at higher temperatures which occurs before the melting of the rest of the duplex. To test this proposal, the diffusion rates, the chemical shifts of the nonexchangeable protons, the linewidths of the imino protons, and the optical absorbance of many DNAs, with and without mismatched sites, have been obtained as a function of temperature.

Additional information is also needed to allow the estimation of the relative contributions of curvature and flexibility to the enhanced diffusion. To do this, the diffusion rates of DNAs with mismatched sites separated by the helical repeat have been examined. In one sample, the mismatches are in phase with respect to the helical repeat and out of phase in the other. The sequences to be studied are depicted in Figure 1. When curved elements are in phase and separated by the helical repeat, the curvature contributions of the two sites to the diffusion rate will largely add together. When curved elements are out of phase and separated by the helical repeat, the curvature contributions will largely cancel out. Purely flexible elements will have the same effect on diffusion whether in or out of phase at any separation. The presence of stable curvature due to the presence of dA tracts was established by comparison of the gel mobilities of DNAs with dA tracts in and out of phase with respect to the helical repeat (*33, 35−38*).

EXPERIMENTAL PROCEDURES

Sample Preparation. The 25mers, whose sequences are given in Figure 1, were obtained from Integrated DNA Technologies Inc., Coralville, IA. The 12mer, d(CGCGAAT-TCGCG), was obtained from DNAgency, Melvern, PA. The DNA samples were ethanol precipitated 3 times to remove salt, trace amounts of protecting groups, and other contaminants. NMR and HPLC-based analysis of the samples showed no detectable impurities.

The single-stranded DNAs were combined to produce duplex DNAs. Once the two strands were combined, the samples were annealed by heating the sample to 80 °C in a water bath and allowing the water to cool to room temperature. The one-dimensional NMR spectra of the resulting samples were examined, and additional titration was carried out until there was no detectable presence of single-strand material.

Each of the 25mer NMR samples contained 27 A_{260} of DNA in 500 μL of 140 mM NaCl, 20 mM perdeuterated Tris buffer at pH 7.0. The 12mer NMR sample consisted of 25 A_{260} of DNA in 500 μL of 100 mM NaCl, 10 mM NaPO$_4$, and 0.05 mM EDTA at pH 7.0. One A_{260} is equivalent to an optical density of 1 at 260 nm in a 1 cm path length cell.

The samples for the optical melting curves contained 1 A_{260} of DNA in 1 mL. The optical melting curves were determined using Hitachi U-2000 and Shimazdu UV-2401PC spectrophotometers. The temperature of the sample was raised at 1 °C per minute, and the samples were equilibrated for 5 min at each temperature before the readings were taken. Three readings of the absorbance were made at each temperature and averaged.

NMR Experiments and Gradient Calibration. All of the diffusion experiments were carried out using a Varian 400 MHz UnityPlus spectrometer and a Nalorac double-resonance, pulsed field gradient, 5 mm probe. The gradient strength calibration was conducted using a spin−echo FID on a sealed, doped ^{2}H$_2$O sample with the *z*-axis gradient on during the acquisition period. The calibration produces a profile of the sample that is a function of sample height and gradient strength.

The diffusion coefficient of ^{2}HOH in ^{2}H$_2$O was determined to validate the gradient calibration method. It was found that the diffusion of ^{2}HOH in ^{2}H$_2$O was 1.867×10^{-5} cm^2/s at 25 °C, which is in agreement with the literature value of 1.870×10^{-5} cm^2/s (*39*). This small discrepancy may be due to the 400 MHz spectrometer being limited to a spectral width of 100 000 Hz that is not sufficient to observe the entire lineshape of the doped water resonance in the gradient calibration procedure.

The diffusion experiments were carried out using the PFG-STE (pulsed field gradient stimulated echo) experiment with

Table 1: Comparison of Diffusion Coefficients, in cm^2/s, with Literature Values[a]

sample	diffusion coefficient (cm^2/s)	diffusion coefficient converted to ^2H_2O value	experimental diffusion coefficient
^2HOH in ^2H_2O	1.870×10^{-5}	1.870×10^{-5}	1.867×10^{-5}
methanol in H_2O	1.580×10^{-5}	1.296×10^{-5}	1.347×10^{-5}
ethanol in H_2O	1.230×10^{-5}	1.071×10^{-5}	1.135×10^{-5}
12mer (scattering) in H_2O	1.341×10^{-6}	1.010×01^{-6}	1.232×10^{-6}
12mer (NMR) in ^2H_2O	1.230×10^{-6}	1.230×10^{-6}	1.232×10^{-6}

[a] All values are at 25 °C. Some of the prior results were obtained in H_2O, and the ^2H_2O column contains the values adjusted for the viscosity difference between H_2O and ^2H_2O. The 12mer DNA is the self-complementary d(CGCGAATTCGCG).

$\delta = 9$ ms and $\Delta = 260$ ms essentially as described previously (*20*). The strengths of the first and third gradient pulses were the same, and the experiment was carried out with 25 different values of gradient strength from 2.5 to 78.9 G/cm (*20*). The strength of the gradient used to suppress transverse magnetization, applied at the middle of the Δ period, was 1.5 G/cm. A total of 5568 complex points were collected, with 20 transients, at 10 °C intervals between 15 and 85 °C. A spectral width of 6999.1 Hz and a delay time of 10 s were used. The free induction decays were Gaussian-weighted, Fourier-transformed, integrated, and base-line-corrected. VNMR version 6.1B software was used to acquire and process the data. A line broadening of 50 Hz was applied to the spectra in order to average the intensity of all resonances in the region selected. The region of the spectrum that contains resonances from the H2′ and H2″ protons, between 1.8 and 3.0 ppm, was used to determine the diffusion coefficients. The regions corresponding to aromatic and to the H1′/H5 protons were also examined and found to give the same results as the H2′/H2″region.

The diffusion coefficients, D, were obtained from the ratio of the intensity obtained with gradient strength G, I_G, to that obtained with no gradient, I_0, by use of $I_G/I_0 = \exp[-D\gamma_{H^2}\delta^2 G^2(\Delta - \delta/3)]$ (*40, 41*). Plots of $\ln(I_G/I_0)$ versus G^2 were fit by nonlinear least squares to obtain the diffusion coefficients D as described previously (*20*), and representative plots are included in the Supporting Information. KaleidaGraph version 3.02, from Synergy Software, was used to graph the results, to carry out the nonlinear least-squares fits, and to calculate the correlation coefficients as previously described (*20*). Seven independent determinations were made of several diffusion coefficients, and the standard deviation of each was in the range of 1−2%. The standard deviation for the determination of a single data point, a particular I_G, was found to be on the order of 1−2%. The plots of the temperature dependence of the structure functions, discussed below, also indicate the reproducibility of the experiments. All of the correlation coefficients (*20*) for the fits of the diffusion coefficients were greater than 0.996. The Supporting Information contains representative plots of $\ln(I_G/I_0)$ versus G^2.

The diffusion coefficients determined by this methodology are compared with those obtained previously by other approaches in Table 1. The diffusion coefficient of ^2HOH in ^2H_2O was determined by pulsed field gradient deuterium NMR (*42*), and those of ethanol and methanol in H_2O were determined by monitoring the diffusion in long capillary
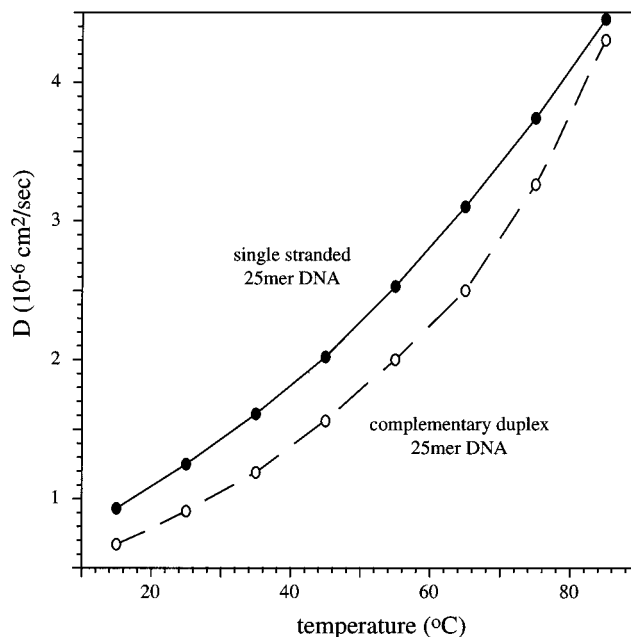

FIGURE 2: Diffusion coefficients of the single-stranded 25mer DNA, d(ACAGGACCGCGATACGCCGGAACGA), and the double-stranded DNA formed from this single strand and its complement are shown as a function of temperature.

tubes (*43, 44*). The diffusion of the duplex formed by the self-complementary d(CGCGAATTCGCG) has been previously determined by light scattering (*45*) and by NMR (*39*). The diffusion coefficients that were obtained in H_2O were converted, to take into account the difference in viscosity between H_2O and ^2H_2O, to allow comparison with the results obtained here on samples in ^2H_2O.

RESULTS AND DISCUSSION

Isolation of the DNA-Specific Component of the Diffusion Coefficient. The focus of this study is the flexibility and curvature induced by the presence of mismatched sites and how these depend on temperature. This cannot be readily deduced directly from the diffusion coefficients, alone, as diffusion in water is a highly temperature-dependent process. The diffusion coefficient of a rigid molecule will increase about 4-fold from 0 to 100 °C due to the temperature dependence of the viscosity of water and a Boltzmann term. By way of contrast, the difference in diffusion coefficients between single- and double-stranded 25mer DNAs is on the order of 50%. The results in Figure 2 show that the diffusion coefficients of both the single-stranded and duplex DNAs increase considerably with increasing temperature. Plots of the diffusion coefficients of additional DNAs and of methanol, ethanol, and dAMP as a function of temperature are included in the Supporting Information. In this mode of presentation, it is difficult to ascertain how the difference in diffusion coefficients between the single-stranded and duplex DNAs changes with temperature.

Thus, the temperature dependence of the diffusion coefficients needs to be separated into the component that depends on changes in the DNA from that common to all molecules. The standard, Einstein's, equation for diffusion is
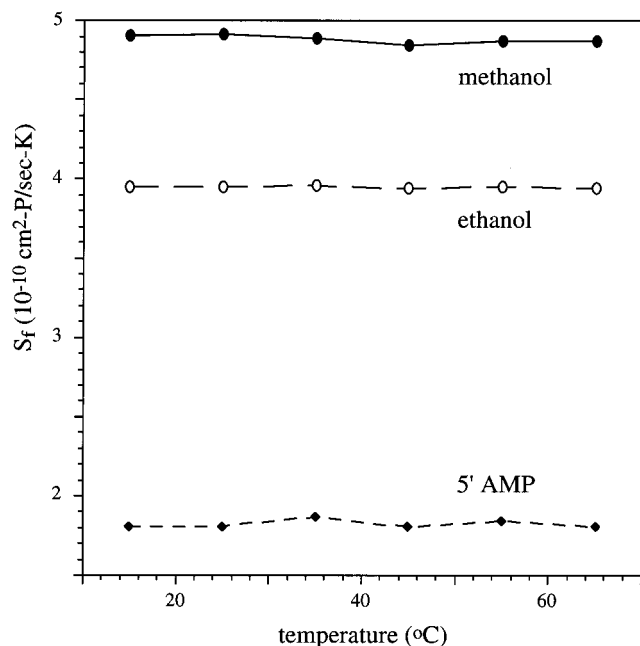
$$D = kT/f_t$$

FIGURE 3: Shape functions, $S_f = \eta D/T$, of methanol, ethanol, and 5'-AMP are shown as a function of temperature.

with D the diffusion coefficient, k Boltzmann's constant, T the absolute temperature, and f_t the frictional coefficient. The frictional coefficient depends on the solvent viscosity, η:

$$f_t = \eta f_s$$

with f_s the shape coefficient. The viscosity of water is temperature dependent (*39*):

$$\log \eta = a + [b/(c - T)]$$

For a 100% H_2O solution, $a = -4.5318$, $b = -220.57$, and $c = 149.39$ and T is in kelvin. For a 100% ^2H_2O solution, $a = -4.2911$, $b = -164.97$, and $c = 174.24$ (*39*). The viscosity of water has only a modest dependence on salt concentration (*39*).

To remove the viscosity and Boltzmann term dependence, we have decided to use the shape function, S_f, which we define as $\eta D/T$. The S_f of methanol, ethanol, and 5'-AMP are plotted as a function of temperature in Figure 3. It is seen that the S_f of 5'AMP, ethanol, and methanol are constant, within a few percent, over the temperature range shown. This is the expected result for molecules whose shape does not change. The temperature independence of the S_f also shows that the field gradients and other experimental parameters are constant over the temperature range needed to study the DNAs containing mismatched sites.

The hydrodynamic properties of duplex DNA can be modeled by a cylinder with a radius of 20 Å and a length of 3.4 Å per base pair (*39, 45–47*). A 25mer duplex will have a length-to-diameter ratio of 4.25, which is the axial ratio. The diffusion of the DNA is dependent on the axial ratio (*39, 45–47*), and the axial ratio will decrease as the flexibility or curvature of the DNA increases. Increases in the flexibility or curvature of a DNA will increase the shape function of the DNA.

Temperature Dependence of the Shape Function of a Fully Complementary Duplex DNA. The shape function of the 25mer fully complementary DNA duplex exhibits a 45%
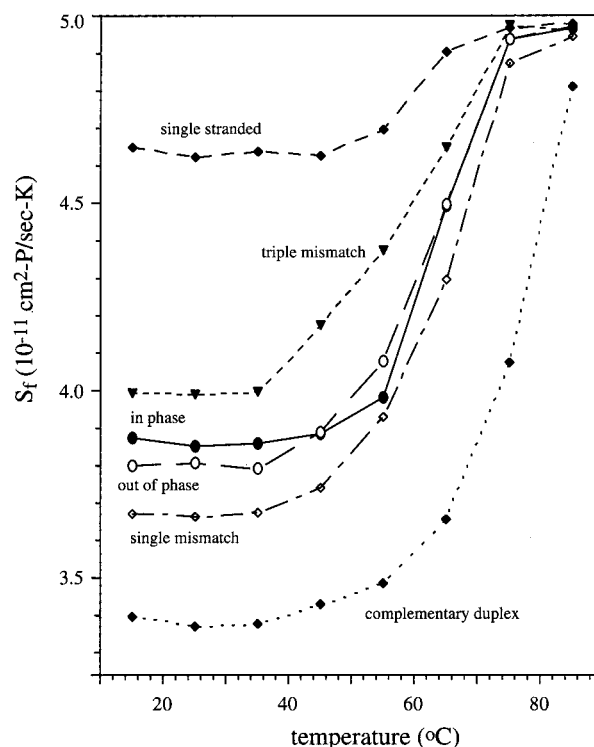

FIGURE 4: Shape functions of the complementary, mismatched, and single-stranded DNAs are shown as a function of temperature. These curves can be considered to be the shape function melting curves of the DNAs.

increase between 15 and 85 °C as shown in Figure 4. The melting curve of the shape function has the same general shape as that of a more familiar optical melting curve. The temperature dependence of the proton chemical shifts of this DNA indicates that the DNA is not completely melted even at 95 °C, as the results in Figure 5 show. When the duplex is completely melted, the proton NMR spectrum of the duplex corresponds to the sum of the spectra of the two single stands. Figure 5 shows the spectra of the two single strands that make up the duplex as well as their sum. It is seen that the spectrum of the duplex is not that of the sum of the spectra of the two single strands at 95 °C. The results in Figures 4 and 5 were obtained with the same sample of the complementary duplex.

These results indicate that the melting of the shape function occurs 15–20 °C, or more, below that of the separation of the two strands that is monitored by the proton chemical shifts. These results are consistent with the proposed model in which the melting of the shape function occurs due to the localized melting, or breathing, of the duplex DNA. The localized melting occurs at lower temperatures than does the complete separation of the two strands. Localized melting also increases the exchange rates of the imino protons with water, and the exchange increases the linewidths of the imino protons. The melting temperature of the shape function, $\sim$75 °C, is similar to that associated with the exchange broadening of the imino protons which is also $\sim$75 °C. The imino proton spectra of the fully complementary duplex DNA have been obtained as a function of temperature and are included in the Supporting Information.

Shape Function of Duplex DNAs with a Single Mismatch. The shape function of the duplex DNA with a single mismatch is about 10% larger than that of the fully
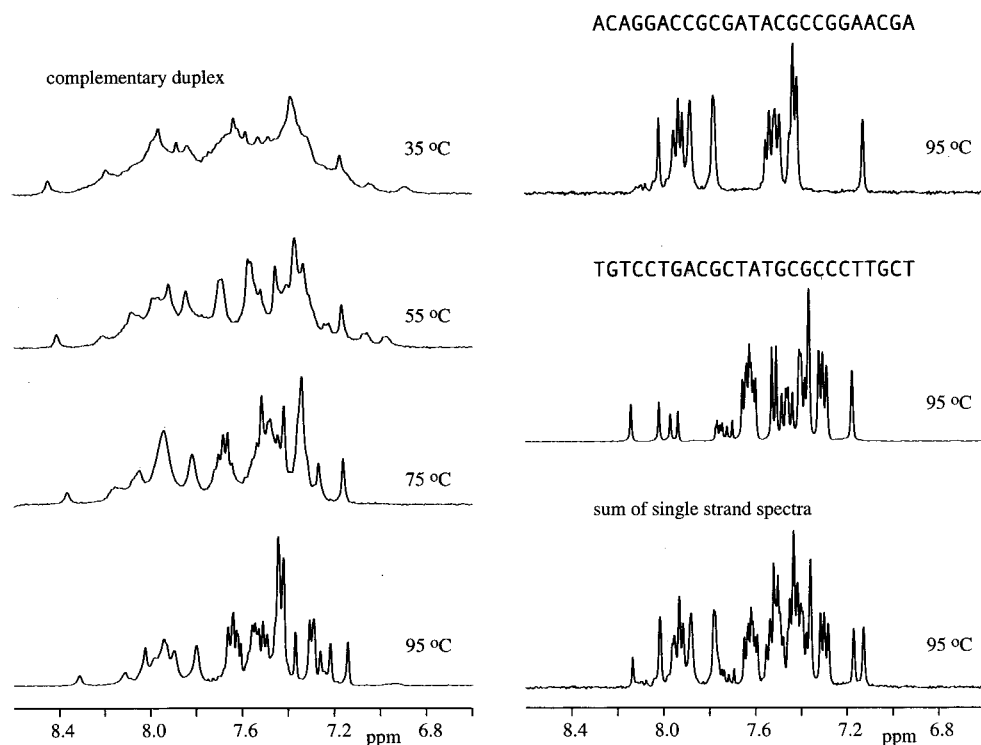
FIGURE 5: Proton NMR spectra of the complementary duplex as a function of temperature are shown on the right. On the left, the proton spectra of the indicated single strands obtained with the samples at 95 °C as well as the sum of these spectra are shown.

complementary duplex DNA at the lowest temperature examined as the results in Figure 4 show. This indicates that a DNA with a single mismatch site is more flexible than the fully complementary DNA at temperatures as low as 15 °C. The shape function of the single mismatch site DNA is constant from about 15 to 40 °C as is that of the fully complementary duplex DNA.

The melting curve of the shape function is largely cooperative, and the melting temperature is between 65 and 70 °C as shown in Figure 4. The melting of this DNA as monitored by the proton chemical shifts is not complete at 95 °C as the results in Figure 7 show. These results indicate that the melting of the shape function occurs 25−30 °C below that of the separation of the two strands as monitored by the proton chemical shifts. The melting of the imino protons, as measured by their linewidths, is close to that of the fully complementary duplex as the results in the Supporting Information show. The imino proton spectra of these samples are not sufficiently resolved to detect the linewidth changes of individual imino protons. The use of samples with strategically placed isotopic labels or 4-thio-uridine residues could allow monitoring of the breathing at selected individual sites.

Similarly, the optical melting temperature of the fully complementary DNA and that of the DNA with a single mismatch differ by only a few degrees as shown in Figure 6. The optical melting temperatures are much lower than those observed in the NMR experiments as the concentrations of the DNAs are 54 times less in the optical experiments and the melting temperature of a duplex DNA is highly concentration dependent (*48*).

Taken together, these results indicate that the presence of a single mismatched site has relatively small effects on the melting temperature of the strand separation of the DNA as
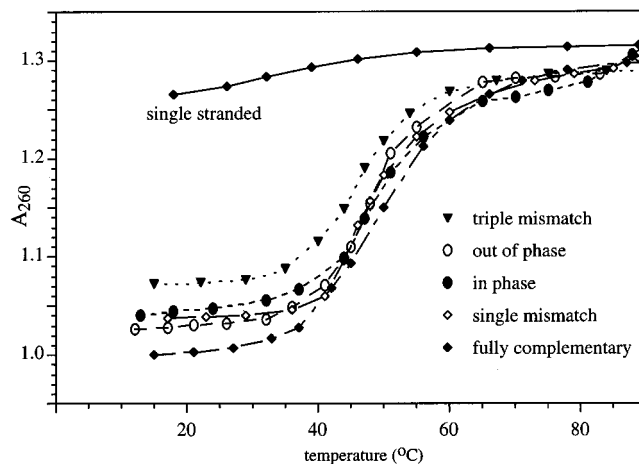

FIGURE 6: Optical melting curves of the complementary, mismatched, and single-stranded DNAs are shown. The absorbance at 260 nm, A_{260}, is plotted as a function of temperature.

monitored by the proton chemical shifts and by optical absorbance. This is in agreement with prior results (*2, 5, 12−14, 23*). A single mismatched site does, however, have a significant effect on the shape function at all temperatures. Over the temperature range of 15−40 °C, the presence of a single mismatched site increases the shape function by about 10% over that of the fully complementary duplex, indicating an increase in flexibility. The shape function of the single mismatch DNA melts about 8 °C lower than that of the fully complementary duplex which is attributed, in part, to localized melting at, and adjacent to, the mismatched site.

Temperature Dependence of the Shape Function of a Triple Mismatch DNA. The same general pattern of results is observed for the duplex with the triple mismatch as for the single mismatch except that the effects are much larger. The duplex with a triple mismatch has a shape function that
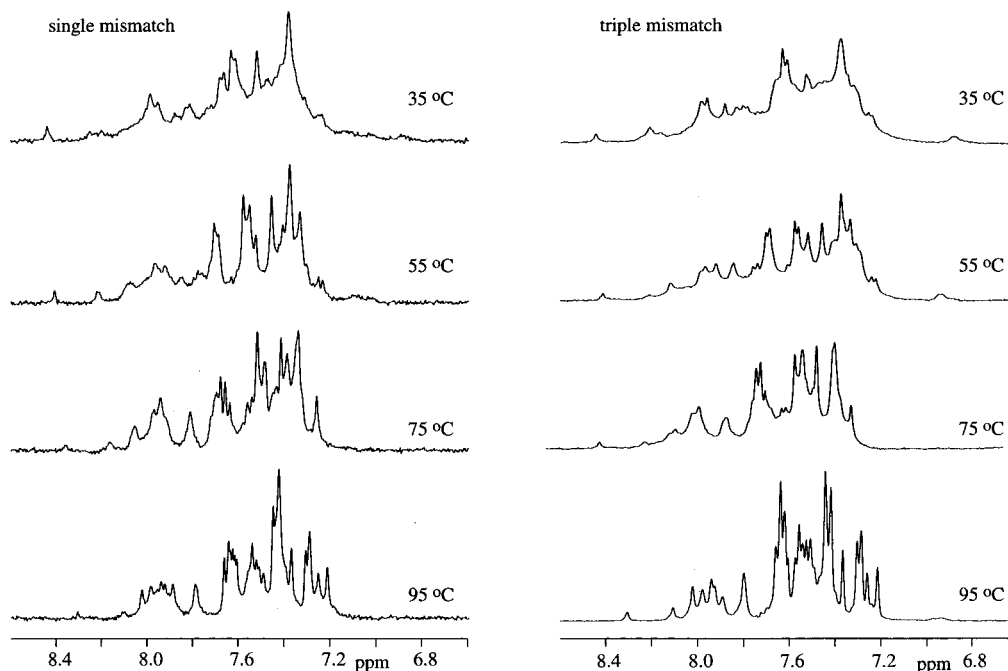
FIGURE 7: One-dimensional proton NMR spectra of the DNA with a single mismatch are shown on the left, and those of the DNA with a triple mismatch are shown on the right. Both sets of spectra were obtained at the indicated temperatures. The spectra were obtained on the same samples as those used to obtain the shape function data.

is almost midway between that of single-stranded and duplex DNA at low temperatures, and the shape function is nearly constant over the range of 15−35 °C. The melting temperature of the triple mismatch DNA duplex is above 95 °C as monitored by the proton chemical shifts, as shown in Figure 7. The melting temperature of the shape function is about 60 °C, as shown in Figure 4. The optical melting temperature of the triple mismatch sample is about 5 °C lower than that of the fully complementary duplex as the results in Figure 6 show. The differences in optical and NMR melting temperatures cannot be directly compared as the concentration dependence of melting is a function of the enthalpy and entropy of duplex formation (*48*), both of which are likely to be different for fully complementary and mismatched DNAs.

Taken together, these results indicate that a triple mismatch has a modest effect on the temperature needed for the separation of the two strands as monitored by the proton chemical shifts and the optical melting. The triple mismatch has a much larger effect on the shape function at all temperatures. At low temperatures, the shape function is about 20% greater than that of the fully complementary duplex DNA. The melting temperature of the shape function is about 15 °C lower than that of the fully complementary DNA. These results indicate that a triple mismatch introduces considerable flexibility to the DNA at low temperatures and that there is localized melting due to the triple mismatch site at temperatures below that of the strand separation of the duplex.

Shape Functions of Duplex DNAs with Mismatch Sites In or Out of Phase with Respect to the Helical Repeat. The general features of the DNAs with mismatch sites in or out of phase with respect to the helical repeat are midway between those of the DNAs with single and triple mismatches as the results in Figures 4 through 7 show. The DNAs containing in phase and out of phase mismatched sites have

shape functions which are about 15% greater than those of the fully complementary duplex DNA at low temperatures. The melting temperatures of their shape functions are about 15 °C less than that of the fully complementary duplex as the results in Figure 4 show. The optical melting curves of the two DNAs with the mismatches separated by the helical repeat are essentially the same, as the results in Figure 6 show. The temperature dependence of the chemical shifts of their nonexchangeable protons is also essentially the same (data not shown). These results indicate that the presence of two mismatched sites, separated by the helical repeat, introduces flexibility which is about halfway between that of single and triple mismatch sites located at the center of the DNA.

The shape function of the DNA with in-phase mismatched sites is larger than that of the DNA with the mismatched sites out of phase over the temperature range of 15−35 °C. This indicates that the mismatched sites have some curvature. Curvature effects will largely add together when the element is in phase with the helical repeat and largely cancel when the element is out of phase with respect to the helical repeat (*33−37*). Flexibility effects will largely add together whether the element is in or out of phase with respect to the helical repeat (*33−37*). The observed difference between the two shape functions, from 15 to 35 °C, is just under 3%, and the presence of a difference between the shape functions of the two DNAs indicates that the dA-dC mismatches have some curvature. As the temperature is raised, the shape functions of the two DNAs become more similar. Additional studies are underway on dA tract DNAs of known curvature. These studies will aid development of the methods to quantify the extent of curvature from shape function data.

Temperature Dependence of the Shape Function of a Single-Stranded DNA. The shape function of the 25mer single-stranded DNA exhibits less than a 10% increase between 15 and 85 °C as shown in Figure 4. The shape

function of the single-stranded DNA is almost 40% greater than that of the duplex DNA at the lowest temperatures examined. The temperature dependence of the chemical shifts of the single-stranded DNA indicates that the DNA has some structure at temperatures up to about 60 °C as the results in Figure 5 show. The single-stranded DNA has several, short self-complementary regions. The increase in the shape function of the single-stranded DNA occurs over the same temperature range as does the complete melting of the single strand as monitored by the proton chemical shifts of the sample.

The optical absorbance of the single-stranded DNA shows a small increase over this temperature range with the maximal hypochromicity observed at 60 °C as shown in Figure 6. The melting of the shape function is more cooperative than that of the optical absorbance. Both melting processes are essentially complete and so is the melting as monitored by the proton chemical shifts, by 60 °C.

Effects of Mismatch Sites on the Flexibility and Curvature of Duplex DNA. The above results indicate that the presence of a single mismatch site increases the shape function, and diffusion coefficient, of duplex DNA at all temperatures studied. The temperature dependence of the shape functions, the optical absorption, and the proton chemical shifts of the DNAs are all consistent with the proposed model. The model attributes localized melting at, and adjacent to, the mismatched site as the origin of the large increase in the flexibility of the DNA that occurs at temperatures below that of strand separation. At low temperatures, the single mismatch acts as a flexible joint. The presence of three consecutive mismatched sites gives rise to a substantially larger increase in the shape function at all temperatures examined than does a single mismatch. The triple mismatch DNA has the largest temperature difference between the overall melting and the transition temperature for the shape function of the DNAs examined here. Comparison of the results on the duplex DNAs that have single mismatched sites in or out of phase with respect to the helical repeat suggests that the dA-dC mismatched sites have modest curvature. Thus, mismatched sites appear to have sufficiently greater flexibility than fully complementary DNA to allow flexibility to be used in their recognition. Localized melting at the mismatched sites can give rise to even greater flexibility. This extra flexibility may alter the interactions of the mismatch site containing DNAs with a wide range of proteins as discussed above.

Additional studies are planned to determine if the local melting in the region near the mismatched site correlates with the melting of the shape function. The local melting can be monitored by the rates of exchange of the imino protons with water. These two-dimensional experiments require much higher concentrations than used for the diffusion experiments.

These methods can be applied to systems other than DNA. For example, the effect of single-site amino acid replacements on the flexibility of proteins, including multidomain proteins, could be examined by the approach presented here as could many aspects of protein folding.

SUPPORTING INFORMATION AVAILABLE

Nine additional figures are available. The first two contain plots of the diffusion coefficients of the small molecule standards and of the DNAs as a function of temperature. There are five figures showing plots of $\ln(I_G/I_0)$ as a function of G^2, one for each of the DNAs. A figure containing the imino proton spectra of the fully complementary DNA, the single mismatch, and the triple mismatch as a function of temperature is included. The final figure shows an expansion of the comparison of the 95 °C spectrum of the fully complementary duplex and that of the sum of spectra of the single strands also obtained at 95 °C (9 pages). This material is available free of charge via the Internet at http://pubs.acs.org.

REFERENCES

1. McDowell, J. A., and Turner, D. H. (1996) *Biochemistry 35*, 14077−14089.
2. Li, Y., Zon, G., and Wilson, W. D. (1991) *Biochemistry 30*, 7566−7572.
3. Lane, A. N., and Peck, B. (1995) *Eur. J. Biochem. 230*, 1073−1087.
4. Kuwata, K., Liu, H., Schleich, T., and James, T. L. (1997) *J. Magn. Reson. 128*, 70−81.
5. Ke, S. H., and Wartell, R. M. (1993) *Nucleic Acids Res. 21*, 5137−5143.
6. Greene, K. L., Jones, R. L., Li, Y., Robinson, H., Wang, A. H., Zon, G., and Wilson, W. D. (1994) *Biochemistry 33*, 1053−1062.
7. Gervais, V., Cognet, J. A., Le Bret, M., Sowers, L. C., and Fazakerley, G. V. (1995) *Eur. J. Biochem. 228*, 279−290.
8. Cognet, J. A., Boulard, Y., and Fazakerley, G. V. (1995) *J. Mol. Biol. 246*, 209−226.
9. Boulard, Y., Cognet, J. A., and Fazakerley, G. V. (1997) *J. Mol. Biol. 268*, 331−347.
10. Boulard, Y., Cognet, J. A., Gabarro-Arpa, J., Le Bret, M., Carbonnaux, C., and Fazakerley, G. V. (1995) *J. Mol. Biol. 246*, 194−208.
11. Borden, K. L., Jenkins, T. C., Skelly, J. V., Brown, T., and Lane, A. N. (1992) *Biochemistry 31*, 5411−5422.
12. Allawi, H. T., and SantaLucia, J., Jr. (1998) *Biochemistry 37*, 2170−2179.
13. Allawi, H. T., and SantaLucia, J., Jr. (1998) *Nucleic Acids Res. 26*, 4925−4934.
14. Allawi, H. T., and SantaLucia, J., Jr. (1997) *Biochemistry 36*, 10581−10594.
15. Modrich, P., and Lahue, R. (1996) *Annu. Rev. Biochem. 65*, 101−133.
16. Modrich, P. (1994) *Science 266*, 1959−1960.
17. Modrich, P. (1997) *J. Biol. Chem. 272*, 24727−24730.
18. Swann, P. F., Waters, T. R., Moulton, D. C., Xu, Y. Z., Zheng, Q., Edwards, M., and Mace, R. (1996) *Science 273*, 1109−1111.
19. Griffin, S., Branch, P., Xu, Y. Z., and Karran, P. (1994) *Biochemistry 33*, 4787−4793.
20. Marathias, V. M., Jerkovic, B., and Bolton, P. H. (1999) *Nucleic Acids Res. 27*, 1854−1858.
21. Freidberg, E. C., Walker, G. C., and Siede, W. (1995) *DNA Repair and Mutagenesis*, ASM, Washington, D.C.
22. Carbonnaux, C., van der Marel, G. A., van Boom, J. H., Guschlbauer, W., and Fazakerley, G. V. (1991) *Biochemistry 30*, 5449−5458.
23. Peyret, N., Seneviratne, P. A., Allawi, H. T., and SantaLucia, J., Jr. (1999) *Biochemistry 38*, 3468−3477.
24. Trotta, E., and Paci, M. (1998) *Nucleic Acids Res. 26*, 4706−4713.
25. Wang, Y. H., Bortner, C. D., and Griffith, J. (1993) *J. Biol. Chem. 268*, 17571−17577.
26. Grove, A., Galeone, A., Mayol, L., and Geiduschek, E. P. (1996) *J. Mol. Biol. 260*, 120−125.
27. Grove, A., Galeone, A., Mayol, L., and Geiduschek, E. P. (1996) *J. Mol. Biol. 260*, 196−206.
28. Bhattacharyya, A., and Lilley, D. M. (1989) *Nucleic Acids Res. 17*, 6821−6840.

29. Travers, A., and Drew, H. (1997) *Biopolymers 44*, 423−433.
30. Thastrom, A., Lowary, P. T., Widlund, H. R., Cao, H., Kubista, M., and Widom, J. (1999) *J. Mol. Biol. 288*, 213−229.
31. Tomonaga, T., Michelotti, G. A., Libutti, D., Uy, A., Sauer, B., and Levens, D. (1998) *Mol. Cell 1*, 759−764.
32. Kahn, J. D., Yun, E., and Crothers, D. M. (1994) *Nature 368*, 163−166.
33. Crothers, D. M. (1998) *Proc. Natl. Acad. Sci. U.S.A. 95*, 15163−15165.
34. Harrington, R. E., and Winicov, I. (1994) *Prog. Nucleic Acid Res. Mol. Biol. 47*, 195−270.
35. Crothers, D. M., Drak, J., Kahn, J. D., and Levene, S. D. (1992) *Methods Enzymol. 212*, 3−29.
36. Hagerman, P. J. (1990) *Annu. Rev. Biochem. 59*, 755−781.
37. Harrington, R. E. (1993) *Electrophoresis 14*, 732−746.
38. Harvey, S. C., Dlakic, M., Griffith, J., Harrington, R., Park, K., Sprous, D., and Zacharias, W. (1995) *J. Biomol. Struct. Dyn. 13*, 301−307.
39. Lapham, J., Rife, J. P., Moore, P. B., and Crothers, D. M. (1997) *J. Biomol. NMR 10*, 255−262.
40. Tanner, J. E., and Stejskal, E. O. (1968) *J. Chem. Phys. 49*, 1768−1777.
41. Tanner, J. E. (1970) *J. Chem. Phys. 52*, 2523−2526.
42. Callaghan, P. T., Le Gros, M. A., and Pinder, D. N. (1983) *J. Chem. Phys. 79*, 6372−6381.
43. Derlacki, Z. J., Easteal, A. J., Edge, A. V. J., Woolf, L. A., and Roksandic, Z. (1985) *J. Phys. Chem. 89*, 5318−5322.
44. Hao, L., and Leaist, D. G. (1996) *J. Chem. Eng. Data 41*, 210−213.
45. Eimer, W., and Pecora, R. (1991) *J. Chem. Phys. 94*, 2324−2329.
46. Garcia de la Torre, J., Navarro, S., and Lopez Martinez, M. C. (1994) *Biophys. J. 66*, 1573−1579.
47. Eimer, W., Williamson, J. R., Boxer, S. G., and Pecora, R. (1990) *Biochemistry 29*, 799−811.
48. Riccelli, P. V., Vallone, P. M., Kashin, I., Faldasz, B. D., Lane, M. J., and Benight, A. S. (1999) *Biochemistry 38*, 11197−11208.